MOLECULAR AND CELLULAR BIOLOGY, Apr. 2000, p. 2865–2873 Vol. 20, No. 8
0270-7306/00/$04.00+0

Defects in Nuclear and Cytoskeletal Morphology and Mitochondrial Localization in Spermatozoa of Mice Lacking Nectin-2, a Component of Cell-Cell Adherens Junctions

MICHAEL J. BOUCHARD,[1] YANGZHANG DONG,[1] BRIAN M. MCDERMOTT, JR.,[1] DU-HUNG LAM,[1] KRISTY R. BROWN,[2] MICHAEL SHELANSKI,[2] ANTHONY R. BELLVÉ,[3,4,5] AND VINCENT R. RACANIELLO[1]*

Departments of Microbiology,[1] Pathology,[2] Anatomy and Cell Biology,[3] and Urology[4] and Center for Reproductive Sciences,[5] Columbia University College of Physicians and Surgeons, New York, New York 10032

Received 12 July 1999/Returned for modification 1 September 1999/Accepted 31 December 1999

Nectin-2 is a cell adhesion molecule encoded by a member of the poliovirus receptor gene family. This family consists of human, monkey, rat, and murine genes that are members of the immunoglobulin gene superfamily. Nectin-2 is a component of cell-cell adherens junctions and interacts with l-afadin, an F-actin-binding protein. Disruption of both alleles of the murine *nectin-2* gene resulted in morphologically aberrant spermatozoa with defects in nuclear and cytoskeletal morphology and mitochondrial localization. Homozygous null males are sterile, while homozygous null females, as well as heterozygous males and females, are fertile. The production by *nectin-2*$^{-/-}$ mice of normal numbers of spermatozoa containing wild-type levels of DNA suggests that Nectin-2 functions at a late stage of germ cell development. Consistent with such a role, Nectin-2 is expressed in the testes only during the later stages of spermatogenesis. The structural defects observed in spermatozoa of *nectin-2*$^{-/-}$ mice suggest a role for this protein in organization and reorganization of the cytoskeleton during spermiogenesis.

The human poliovirus receptor (Pvr) is a member of the immunoglobulin superfamily of proteins (38) and consists of an NH_2-terminal signal sequence, three extracellular immunoglobulin (Ig)-like domains, a transmembrane domain, and a cytoplasmic tail. Pvr was identified by its ability to confer poliovirus susceptibility to receptor-negative cells (23). Sequence homologs of *pvr* were subsequently identified in humans (*pvr*-related receptor 1 [*prr1*] and *prr2* [8, 21]), monkeys (*agm1* and *agm2* [18]), mice (*prr1* and *mph*/*prr2* [murine *pvr* homolog] [24]), and rats (*pE4* [7]). Only *pvr*, *agm1*, and *agm2* encode proteins that can function as cell receptors for poliovirus (18, 23; V. Racaniello, unpublished data, 1999). Pvr, Prr1, Prr2, and Mph/murine Prr2 are entry cofactors for alphaherpesviruses (9, 37).

The cellular functions of members of the Pvr protein family are not known. Some members of the Ig superfamily are involved in cell-cell and cell-extracellular matrix interactions, and others are receptors for cytokines and growth factors. Expression of human Prr2 or Mph/murine Prr2 in cultured cells leads to aggregation, suggesting that these proteins are homophilic adhesion molecules (1, 20). The cytoplasmic domains of Prr1 and Prr2 proteins interact with l-afadin, an actin filament-binding protein (35). l-Afadin is ubiquitously expressed but is localized at specialized membrane structures, called adherens junctions, which are involved in cell-cell adhesion (22). l-Afadin contains one PDZ domain through which it interacts with a COOH-terminal amino acid motif of Prr1 and Prr2 as well as an actin filament-binding domain. Thus, Prr1 and Prr2 are linked to the cytoskeleton through l-afadin. The Prr1 and Prr2 proteins have been renamed Nectin-1 and Nectin-2 (35); the new terminology is used in this paper.

* Corresponding author. Mailing address: Department of Microbiology, Columbia University College of Physicians and Surgeons, 701 W. 168th St., New York, NY 10032. Phone: (212) 305-5707. Fax: (212) 305-5106. E-mail: vrr1@columbia.edu.

To provide information on the function of Pvr family members, we disrupted the murine *nectin-2* gene. Male mice lacking both alleles of *nectin-2* are infertile and produce morphologically aberrant spermatozoa. Heterozygous males and females and homozygous null females are fertile and have no overt developmental defects. The heads of spermatozoa from *nectin-2*$^{-/-}$ mice contain mitochondria, dense outer filaments, and misshapen nuclei, and the mitochondrial sheath of the middle piece is disorganized. These morphological defects may result from an overall disruption of cytoskeletal structure. In normal mice, Nectin-2 is expressed in the testes only during the later stages of spermatogenesis, during which the morphological transformations that produce spermatozoa from the round spermatid occur. Signaling through Nectin-2 may be crucial for the cytoskeletal organization and reorganization that occur during spermiogenesis.

MATERIALS AND METHODS

Generation of mice lacking Nectin-2. A genomic fragment was isolated from a Supercos1::129SVJ genomic library (Stratagene) by hybridization with a radiolabeled probe generated from the cDNA of *nectin-2* (24). Exon 3 (which encodes amino acids 151 to 250 of Nectin-2) was disrupted by inserting a gene encoding neomycin resistance between a *Mun*I and a *Bam*HI site (Fig. 1A). Relative to the endogenous locus, the final construct, pPNT1-3, contains only the 5′ end of exon 3 and, after a deletion of ~1 kb, 9.5 kb of the genomic sequence; the majority of exon 3 and the 5′ splice site of the downstream intron have been deleted (Fig. 1A). Targeted embryonic stem (ES) cells can be identified by the loss of the *Mun*I site in *nectin-2* exon 3 and the gain of a *Pst*I site (Fig. 1B). Three different ES cell lines (CCE, PJ5 [14], and R1 [27]) were used. All cell lines were maintained on mitotically inactivated mouse embryonic fibroblasts (31). ES cells were electroporated with linearized pPNT1-3 and selected with Geneticin and Gancyclovir. Of the 600 CCE, 117 PJ5, and 321 R1 ES cell colonies that survived dual selection, three clones (one CCE, two PJ5, and one R1) had undergone a homologous recombination event. Chimeric male mice that were generated from the injection of targeted ES cell lines into C57BL blastocysts were mated with C57BL females. Their progeny were observed for transmission of agouti coat color (6). Mice derived from the injection of the R1 ES cell clone gave rise to male germ line transmitters. Tail-derived genomic DNA from agouti progeny of this mating was analyzed by Southern blot hybridization to identify mice that were heterozygous for the targeted inactivation of *nectin-2* (11).

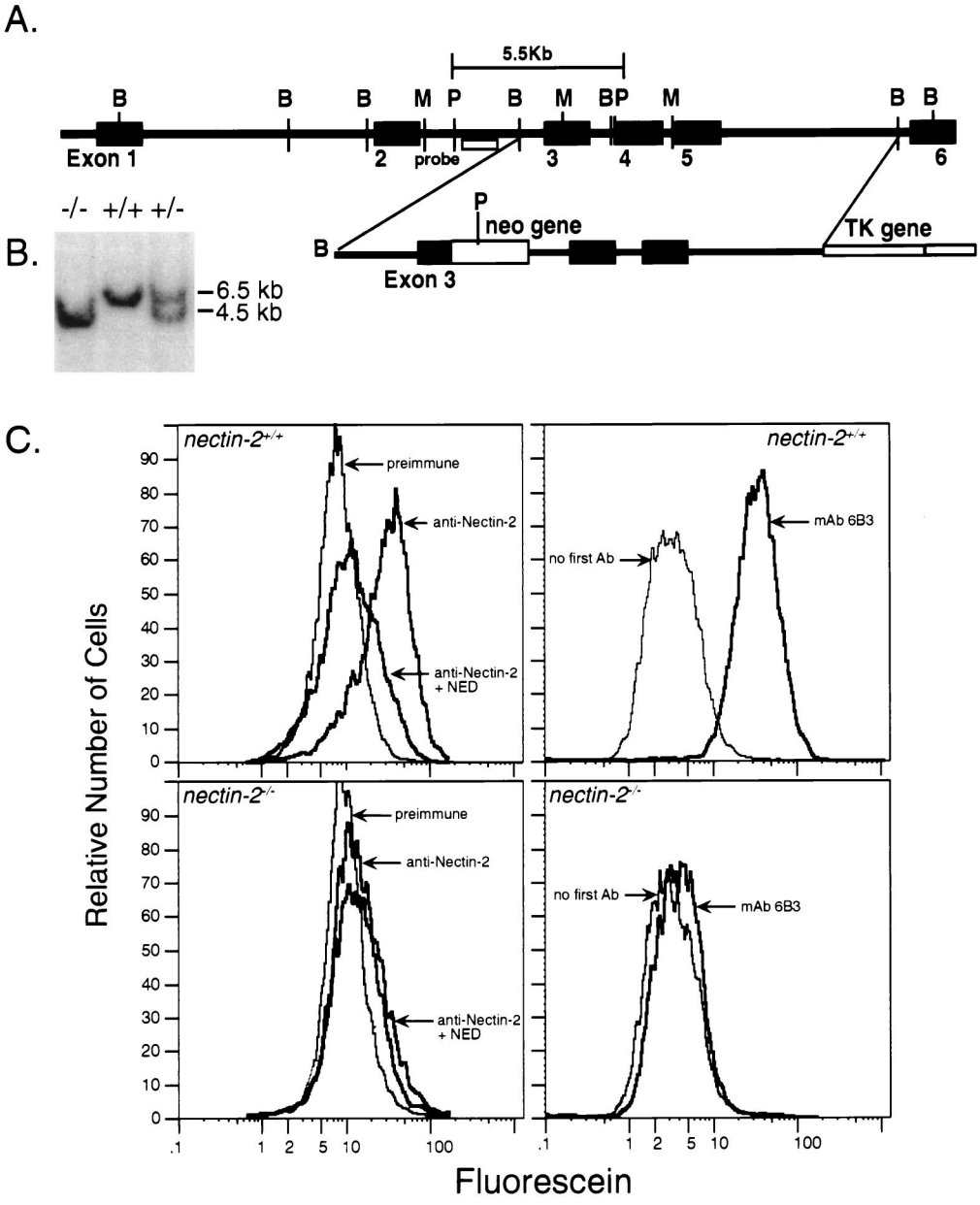

FIG. 1. (A) *nectin-2* exon 3 targeting construct as it would appear after linearization. The genomic locus of *nectin-2* is shown at the top (adapted from reference 24). Restriction fragment sizes are approximate. Black boxes represent exons, and intervening black lines represent introns. The open box at the 3′ end of the targeting construct is nonhomologous DNA from the vector used to generate the targeting construct. The neomycin resistance (neo) gene contains more than one *Pst*I site, but only the first, which decreases the size of the exon 3 genomic fragment after targeting, is shown. B, *Bam*HI; P, *Pst*I; M, *Mun*I; TK, thymidine kinase gene. (B) Southern blot analysis of tail DNA from mice that were wild type (*nectin-2*$^{+/+}$), heterozygous for the *nectin-2* disruption (*nectin-2*$^{+/-}$), or homozygous for the disruption (*nectin-2*$^{-/-}$). Genomic DNA was digested with the restriction enzyme *Pst*I. The hybridization probe used (shown in panel A) can detect a change in the size of the *Pst*I genomic fragment that would result from the disruption of *nectin-2*. DNA marker sizes and positions are indicated. (C) Flow-cytometric analysis of Nectin-2 expression on primary kidney cell cultures derived from *nectin-2*$^{+/+}$ mice (top panels) and *nectin-2*$^{-/-}$ mice (bottom panels). Analyses with rabbit preimmune serum (preimmune), rabbit anti-Nectin-2 polyclonal serum (anti-Nectin-2), and serum that was preincubated with excess NED are shown in the two left panels. Analyses with or without rat anti-Nectin-2 monoclonal antibody (mAb) 6B3 are shown in the two right panels. Bovine serum albumin did not compete away the reactivity of rabbit anti-Nectin-2 polyclonal serum with *nectin-2*$^{+/+}$ kidney cells (Dong and Racaniello, unpublished data). Ab, antibody.

Determination of sperm count and motility. The epididymides and vasa deferentia were removed, cut into 2-mm-long pieces, resuspended in a buffer containing 75 mM NaCl and 24 mM EDTA, and homogenized to dissociate somatic cells. The sperm remaining as a monodispersed suspension were counted by hemacytometry. The total number of sperm in the original sample was calculated after correcting for sample volume and tissue weight. Motility of sperm obtained from the epididymides and vasa deferentia was observed as described elsewhere (3).

Nectin-2 mRNA expression. A cDNA clone encoding Nectin-2δ, reported to be a secreted form of the protein (2), was obtained from Akio Nomoto. Expression of *nectin-2*δ cDNA in cultured cells failed to yield either secreted or membrane-bound protein. Nucleotide sequence analysis of *nectin-2*δ cDNA revealed that it lacked the initiating AUG codon and the next 7 amino acids. The defect was corrected by mutagenesis, and the resulting *nectin-2*δ cDNA was able to direct the expression of Nectin-2δ on the plasma membranes of cultured cells. We conclude that *nectin-2*δ mRNA encodes a membrane-bound protein. A similar conclusion has been reached by others who used Western blot analysis with antibodies specific for Nectin-2α and Nectin-2δ (35).

Flow cytometry. Expression of surface antigens was determined by fluorescence-activated cell sorter (FACS) analysis as previously described (25). A rabbit

anti-Nectin-2 polyclonal antiserum was generated against the purified Nectin-2 extracellular domain (NED) (Y. Dong and V. Racaniello, unpublished data) by Cocalico Biological Inc. (Reamstown, Pa.), and the anti-Nectin-2 monoclonal antibody 6B3, which recognizes domain 1 of Nectin-2 (1), was a gift of Akio Nomoto. Mouse primary kidney cell cultures were generated as previously described (30). To ensure the specificity of the polyclonal antiserum, samples of antibody were also incubated with excess NED (1 mg of NED per ml of antiserum) prior to use in FACS analysis of Nectin-2-expressing and -nonexpressing mouse primary kidney cells. Polyclonal antiserum was incubated with bovine serum albumin as a negative control. For analysis of sperm DNA content, sperm were removed from the epididymides and vasa deferentia and counted with a hemacytometer. Approximately 2×10^6 sperm were fixed in 80% ethanol; stained in a solution containing 0.5 mg of propidium iodide, 0.2% NP-40, and 0.5 mg of RNase A; and subjected to FACS analysis.

Isolation of spermatids. Seminiferous tubules were cut into 3-mm^2 fragments and incubated in enriched Krebs-Ringer bicarbonate (EKRB) buffer (4) for 3 h at 32°C, which caused the release of a small number of spermatids from the tubules. After being filtered through 85-μm-pore-size Nitex mesh to remove clumps, spermatids were stained with fluorescein isothiocyanate-conjugated monoclonal antibody 6B3. Staining was detected by fluorescence microscopy.

Staining of tissue sections. Mice were perfused with a solution consisting of 1% acrolein, 13% collidine, and 2.5% glutaraldehyde (3). The testes were removed, paraffin embedded, and sectioned at 4 μm thick. Sections were stained with hematoxylin and eosin and photographed by light microscopy. For immunohistochemistry studies, sections were blocked with 10% serum in phosphate-buffered saline for 30 min and incubated with affinity-purified rabbit anti-Nectin-2 antibody for 45 min. After three washes with PBS, the slides were incubated with a 5-μg/ml solution of biotinylated anti-rabbit antibody (Vector Laboratories, Inc., Burlingame, Calif.) for 30 min, washed three times with PBS, stained with β-galactosidase–avidin (Vector Laboratories), and developed with X-Gal (5-bromo-4-chloro-3-indolyl-β-D-galactopyranoside) as described previously (41).

Electron microscopy. Spermatozoa were isolated as described above, fixed immediately in 2.5% glutaraldehyde–130 mM sodium cacodylate buffer for 1 h, washed with 130 mM cacodylate buffer, and treated with 1% osmicite in 130 mM cacodylate buffer at room temperature. After being washed three times with 130 mM cacodylate buffer, sperm were incubated with 1% tannic acid in 500 mM sodium cacodylate for 30 min at room temperature, washed twice with 100 mM sodium cacodylate, and dehydrated in 50% ethanol for 5 min. Sperm were next incubated with 4% uranyl acetate in 70% ethanol for 1 h at room temperature and then dehydrated in 70, 95, and 100% ethanol in series. Sperm were embedded in LX-112 resin (Ladd), sectioned at about 60 nm, and stained with 4% uranyl acetate and lead citrate. Sections were examined with a Jeol JEM-1200 EXII electron microscope.

MitoTrack and rhodamine phalloidin staining. Sperm were isolated as described above, incubated with 50 nM MitoTrack (Molecular Probes) in EKRB buffer for 45 min at 37°C, and examined by fluorescence microscopy. For F-actin staining, sperm were fixed in acetone for 5 min, incubated with 80 nM rhodamine phalloidin (Cytoskeleton, Inc.) in phosphate-buffered saline containing 10% goat serum, and examined by fluorescence microscopy.

RESULTS

Male mice that lack Nectin-2 are infertile. To determine the cellular function of the Pvr-related family of proteins, we inactivated *nectin-2* in mouse ES cells by targeted mutagenesis and generated Nectin-2-deficient mice. We constructed a targeting vector that would disrupt exon 3 of *nectin-2* (Fig. 1A) and introduced the vector into ES cells. Cell lines that had undergone a targeting event were used to generate mice that transmitted the disrupted gene. These mice were mated to produce *nectin-2*$^{+/-}$ mice. Intercrosses yielded offspring (~30 litters) that segregated with the expected Mendelian frequency: 58 wild type, 127 heterozygotes (*nectin-2*$^{+/-}$), and 51 homozygotes (*nectin-2*$^{-/-}$). Inheritance of the targeted gene was monitored by Southern blot analysis (Fig. 1B).

Transcripts of the *nectin-2* gene are expressed at high levels in the mouse kidney (24). Primary cultures of kidney cells from *nectin-2*$^{+/+}$ and *nectin-2*$^{-/-}$ mice (30) were analyzed by flow cytometry for cell surface expression of Nectin-2 protein (Fig. 1C). Whereas the kidney cells of *nectin-2*$^{+/+}$ mice showed high levels of Nectin-2 expression, the protein was not detected on kidney cells from *nectin-2*$^{-/-}$ mice. A slight reactivity was observed with the rabbit anti-Nectin-2 polyclonal antiserum compared to preimmune serum, but this binding was not competed by the soluble extracellular domain of Nectin-2 (NED), demonstrating that it was due to nonspecific antibodies in the immune serum. In contrast, the fluorescence observed with *nectin-2*$^{+/+}$ kidney cells was competed by NED to levels observed with *nectin-2*$^{-/-}$ cells. These results indicate that Nectin-2 is not produced in *nectin-2*$^{-/-}$ mice.

TABLE 1. Sperm counts and weights of testes and epididymis in male *nectin-2*$^{+/+}$ and *nectin-2*$^{-/-}$ mice[a]

Mouse *nectin-2* genotype	Mean sperm count (10^6) ± SD[b]	Mean wt ± SD of:	
		Testis	Epididymis
nectin-2$^{+/+}$	28.8 ± 1.7	92.7 ± 2.9	46.5 ± 1.8
nectin-2$^{-/-}$	27.7 ± 1.2	94.3 ± 3.0	46.0 ± 2.1

[a] Four mice of each genotype were used per experiment.
[b] Sperm were collected from the epididymides and vas deferentia as described in Materials and Methods. Sperm from *nectin-2*$^{-/-}$ mice were motile, as determined by the method described in reference 3.

Homozygous mutant (*nectin-2*$^{-/-}$) mice did not display any overt developmental abnormalities. However, intercrosses between *nectin-2*$^{-/-}$ mice failed to produce progeny. Male and female *nectin-2*$^{+/-}$ and female *nectin-2*$^{-/-}$ mice are fertile, but *nectin-2*$^{-/-}$ male mice are infertile. When 25 *nectin-2*$^{-/-}$ male mice were mated with wild-type female mice, copulation plugs were identified, showing that mating had occurred, but no pregnancies were observed.

Mice lacking Nectin-2 have defects in spermiogenesis. We examined spermatozoa of *nectin-2*$^{-/-}$ mice to determine the basis of the observed infertility. No differences between the numbers of sperm from the epididymides and vasa deferentia of *nectin-2*$^{+/+}$ and *nectin-2*$^{-/-}$ mice were observed (Table 1). Spermatozoa from *nectin-2*$^{-/-}$ mice are motile but morphologically abnormal. The heads are misshapen, the acrosome and nucleus are heterogeneous in appearance, and frequently the middle piece is thinner and more undulate than that of wild-type sperm (Fig. 2A and B). Sperm from *nectin-2*$^{-/-}$ mice contain the same amount of DNA as wild-type sperm (Fig. 2C), indicating that they have completed meiosis.

The sizes and weights of the testes from *nectin-2*$^{+/+}$ and *nectin-2*$^{-/-}$ mice are similar (Table 1). Histological analyses of testes from *nectin-2*$^{-/-}$ mice did not reveal abnormalities in Leydig, peritubular (V. Racaniello, unpublished data), or Sertoli cells (Fig. 2D to G). Spermatogonia, spermatocytes, and spermatids (spermiogenesis steps 1 to 10) were normal, but at steps 11 to 16 of spermiogenesis, in essentially all nuclei were observed defects involving irregular shapes and prominent translucent vesicles (Fig. 2F and G). The presence of abnormal spermatids, and not spermatocytes, indicates that *nectin-2*$^{-/-}$ mice have defects in spermiogenesis.

Abnormal nuclear morphology and outer dense fiber and mitochondrial localization in spermatozoa of mice lacking Nectin-2. Electron microscopy was used to determine the structural basis for the observed defects in spermatozoa of *nectin-2*$^{-/-}$ mice. Four distinct abnormalities were observed (Fig. 3). First, mitochondria are present in the heads of *nectin-2*$^{-/-}$ spermatozoa. Mitochondria are normally located in the middle piece, but not the head, of a wild-type spermatozoan. Second, although the chromatin is condensed, as in spermatozoa from wild-type mice, the nucleus is distorted. Third, mitochondria in the middle piece are disorganized and do not form the tightly packed helical sheath observed in normal sperm. Fourth, the outer dense fibers are jumbled and extend into the

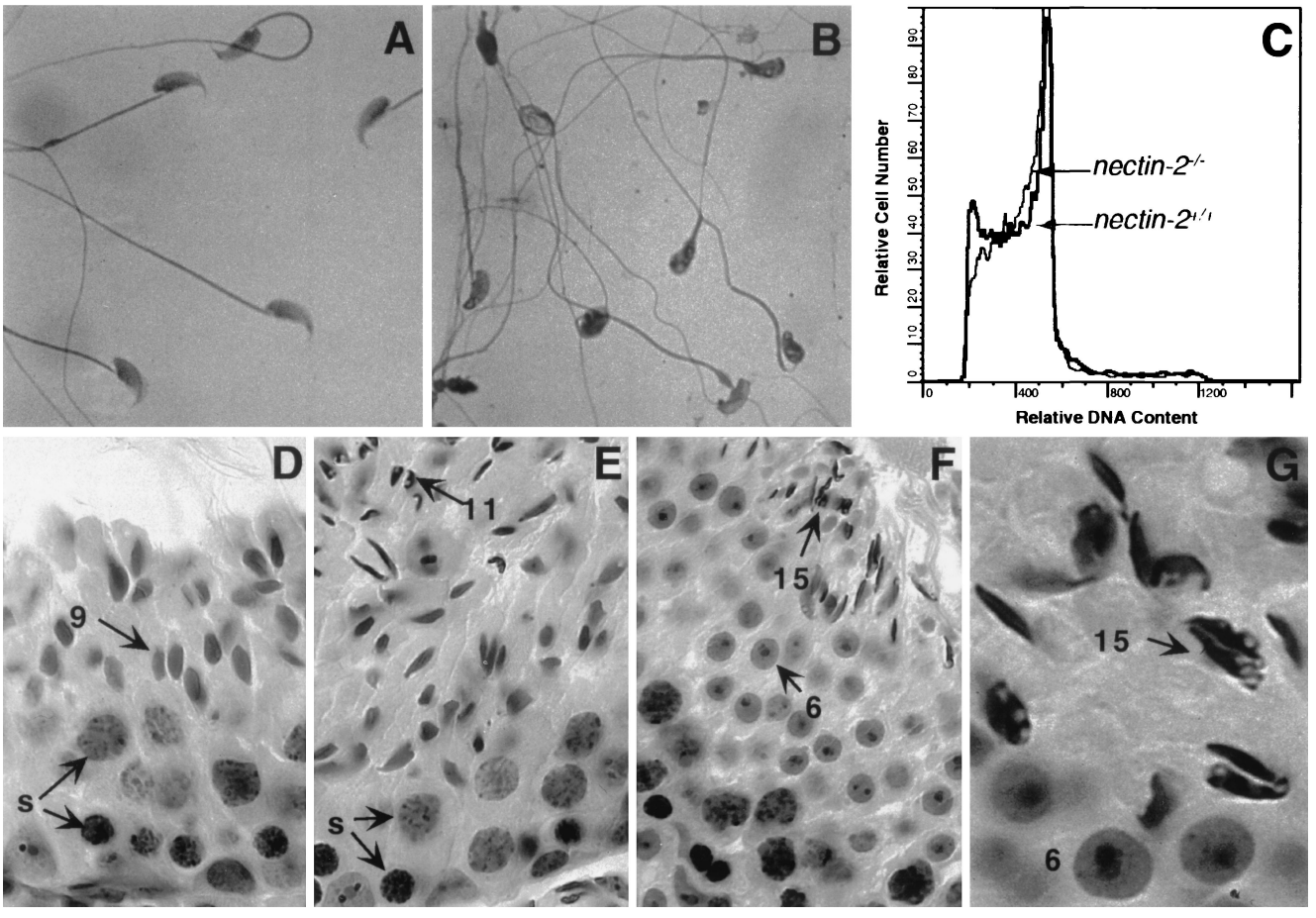

FIG. 2. Phenotype of germ cells in *nectin-2*$^{-/-}$ mice. (A and B) Photomicrograph of sperm from the epididymides and vasa deferentia of *nectin-2*$^{+/+}$ (A) and *nectin-2*$^{-/-}$ (B). mice. Mutant sperm have nuclei with irregular shapes and prominent vesicles, as well as undulate tails. (C) Flow-cytometric analyses of spermatozoa stained with propidium iodide. Only the peak corresponding to 1N cells is present. (D to G) Photomicrographs of paraffin-embedded, hematoxylin- and eosin-stained sections of testes from *nectin-2*$^{-/-}$ mice depicting different stages of the cycle of the seminiferous epithelium, identified by applying classical criteria (32). Present are Sertoli cells, primary spermatocytes, and spermatids at different stages of spermiogenesis: stage IX with normal preleptotene spermatocytes (s), pachytene spermatocytes (s), and step 9 spermatids (arrowed 9) (D); stage XI with normal preleptotene (lower layer) and pachytene (s, middle layer) spermatocytes but aberrant step 11 spermatids (arrowed 11, top left) (E); stage VI with normal spermatids at step 6 (arrowed 6, middle layer) and abnormal spermatids at step 15 (arrowed 15, upper layer), depicting aberrant nuclear shape (top right) (F); and stage VI with normal step 6 spermatids (arrowed 6, bottom) and abnormal step 15 spermatids (arrowed 15, upper layer (G). The latter cells exhibit aberrant nuclear shape and translucent vesicles. Magnifications, ×770 (A), ×684 (D to F), and ×1,995 (G).

head. In normal spermatozoa, outer dense fibers surround the axoneme in the middle and principal pieces.

To determine the proportion of spermatozoa from *nectin-2*$^{-/-}$ mice that contain mitochondria in the head, spermatozoa were stained with MitoTrack Green, a dye that enters cells and selectively binds to mitochondria (Fig. 4). Spermatozoa from wild-type mice were stained only in the middle piece (Fig. 4A). By contrast, about 60% ± (mean ± standard error) 10% of spermatozoa from *nectin-2*$^{-/-}$ mice were stained in the head. In most cases, these spermatozoa were also stained in the middle piece. Some spermatozoa from *nectin-2*$^{-/-}$ mice stained only in the head (<10%), or in the head and in a bulged region in the middle piece (<10%). About 40% of spermatozoa from *nectin-2*$^{-/-}$ mice stained only in the middle piece, a staining pattern observed in spermatozoa from wild-type mice.

Expression of Nectin-2 in testis and spermatozoa. Because mice lacking *nectin-2* have defects in spermiogenesis, we examined expression of this gene in testes. Two *nectin-2* mRNAs derived by alternative splicing have been described. *Nectin-2*α mRNA encodes a membrane-bound form (24), and *nectin-2*δ mRNA reportedly encodes a secreted form of the protein (2). Our results indicate that *nectin-2*δ mRNA encodes a membrane-bound protein (Dong and Racaniello, unpublished data). Nectin-2α and Nectin-2δ proteins have identical extracellular domains but differ in the transmembrane domain and cytoplasmic tail. Both *nectin-2*δ and *nectin-2*α are expressed in testis, although *nectin-2*δ levels are much higher than those of *nectin-2*α (Dong and Racaniello, unpublished data).

Nectin-2 protein expression in testes was examined by immunohistochemistry analyses. Sixteen steps of mouse spermiogenesis have been proposed based on formation of the acrosome and flagellum, nuclear morphology, and mitochondrial location of spermatids. Round spermatids comprise the first eight steps of spermiogenesis. Steps 9 to 16 of spermiogenesis consist of elongated and condensed spermatids (32). Nectin-2 protein was detected in step 9 and step 15 spermatids (Fig. 5F and G). These results indicate that expression of Nectin-2 commences in step 9 spermatids.

The localization of Nectin-2 on isolated spermatids and spermatozoa was also studied. Nectin-2 was detected on the dorsal curvature of isolated condensing spermatids (Fig. 5D

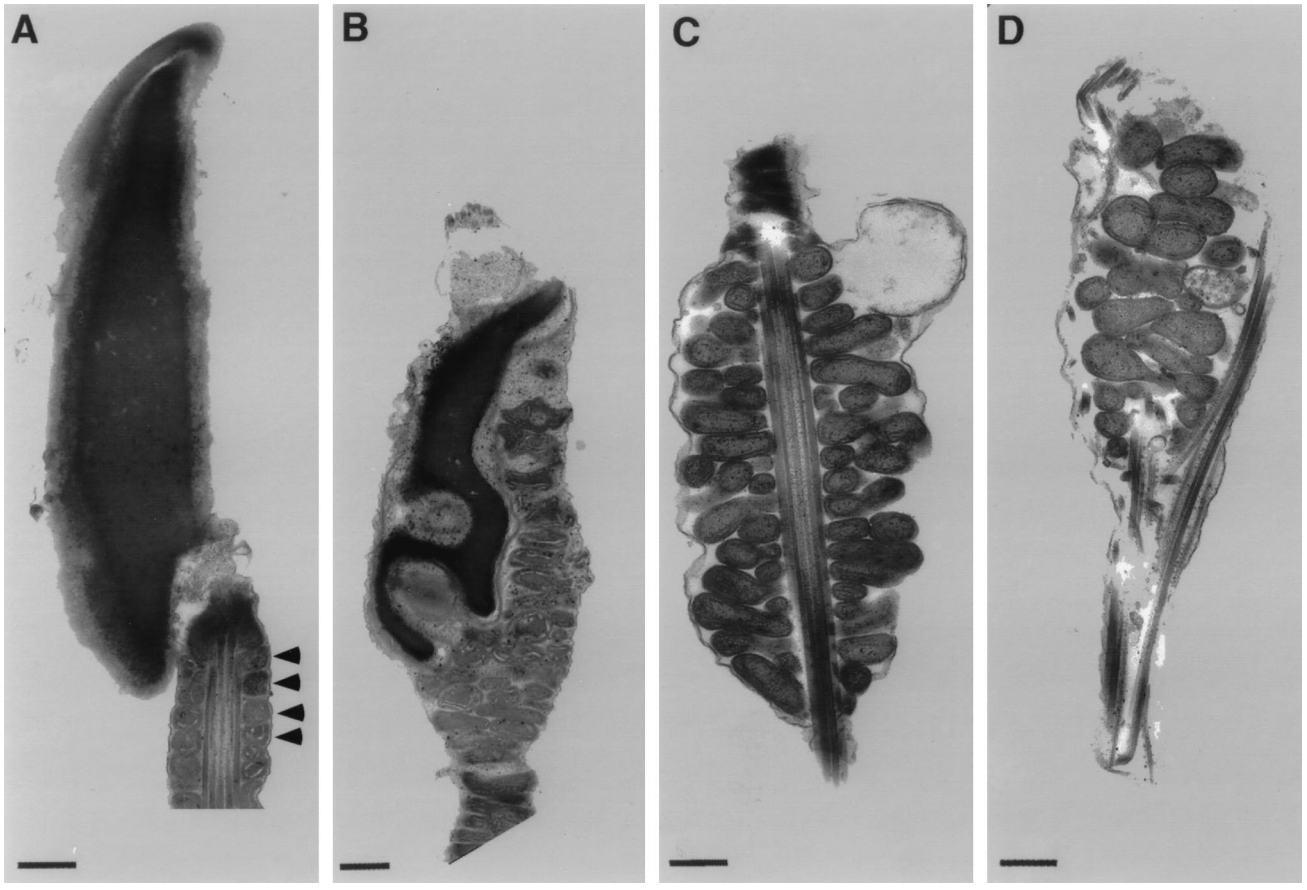

FIG. 3. Ultrastructure of spermatozoa from wild-type and *nectin-2*$^{-/-}$ mice. Electron micrographs of spermatozoa from the epididymides and vasa deferentia of *nectin-2*$^{+/+}$ (A) and *nectin-2*$^{-/-}$ (B to D) mice. (A) Head and middle piece. Arrowheads indicate the mitochondrial helical sheath. (B) Head containing mitochondria and deformed nucleus. (C) Deformed mitochondrial helical sheath. (D) Head containing mitochondria and abnormal outer dense fibers. Bars = 500 nm.

and E) and primarily on the middle piece of wild-type spermatozoa (Fig. 5A). As expected, Nectin-2 expression was not detected in spermatozoa (Fig. 5B) or seminiferous tubules (Fig. 5H) from *nectin-2*$^{-/-}$ mice.

Detection of F-actin in spermatozoa. It has been reported that Nectin-2 is linked to F-actin through l-afadin (35). To determine if the lack of Nectin-2 causes abnormalities in the actin cytoskeleton, spermatozoa were stained with rhodamine

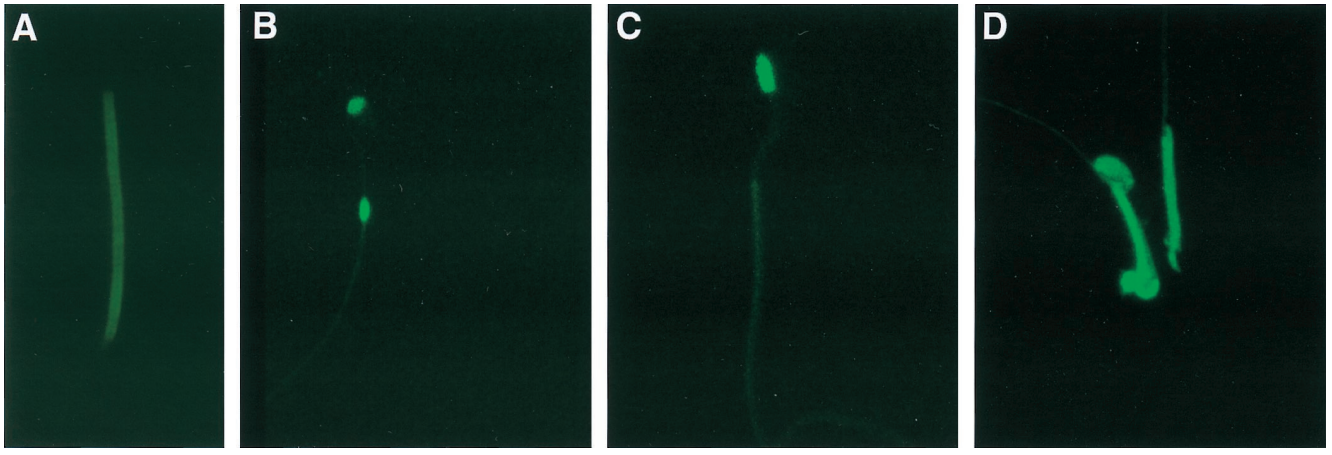

FIG. 4. Localization of mitochondria in spermatozoa by MitoTrack staining. (A) Spermatozoa from wild-type mice showing fluorescence in the middle piece. (B) Spermatozoa from *nectin-2*$^{-/-}$ mice with fluorescence in the head and in a bulge located in the middle piece. (C) Spermatozoa from *nectin-2*$^{-/-}$ mice exhibiting fluorescence only in the head. (D) Spermatozoa from *nectin-2*$^{-/-}$ mice. One cell has fluorescence only in the middle piece, and the other has fluorescence in both the head and the middle piece. Magnifications, ×3,080 (A) and ×1,540 (B to D).

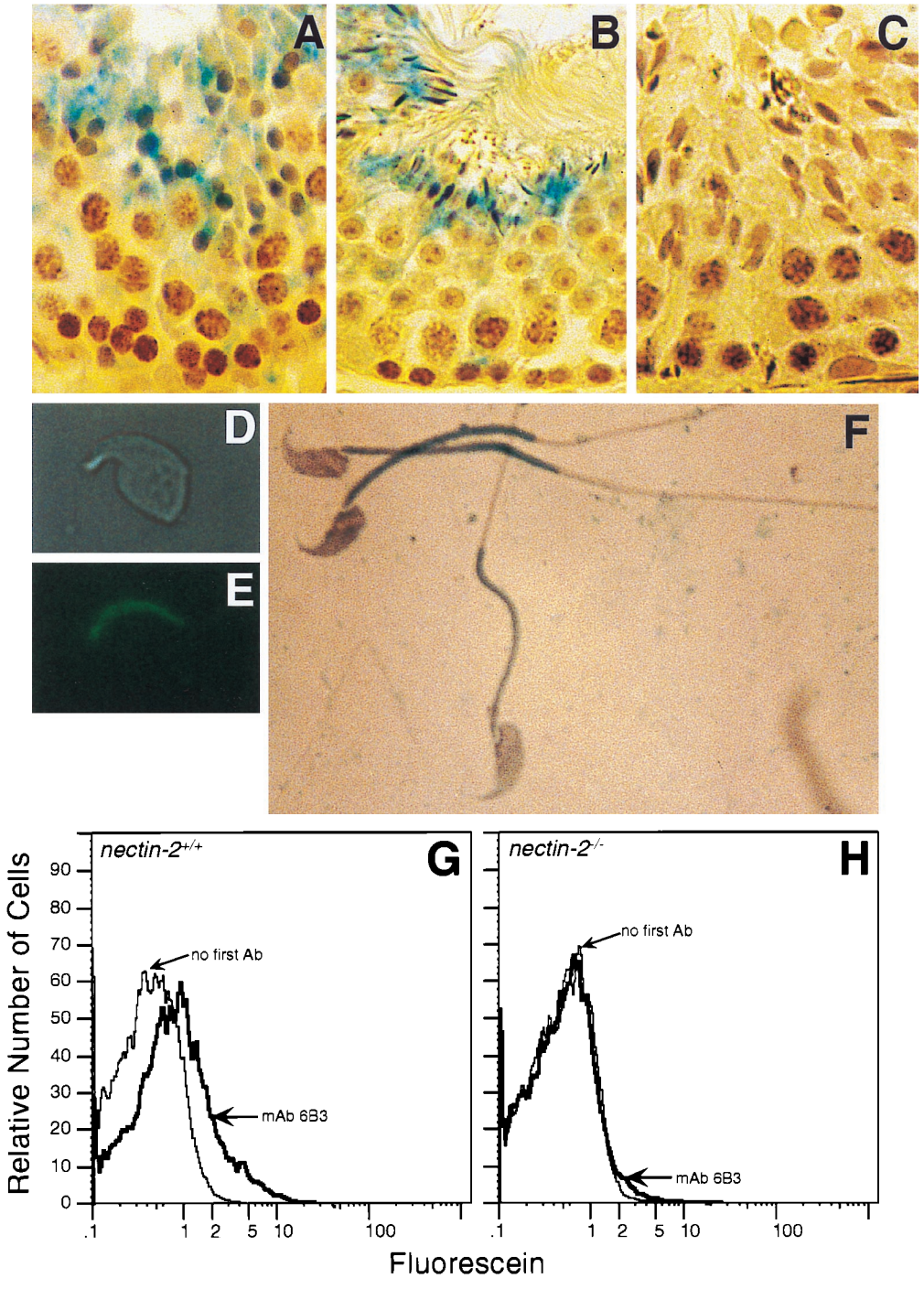

FIG. 5. Expression of Nectin-2 in germ cells. (A to C) Staining of seminiferous tubules from *nectin-2*$^{+/+}$ (A and B) and *nectin-2*$^{-/-}$ (C) mice with affinity-purified rabbit anti-Nectin-2 antibody. Bound antibody was detected by incubation with biotinylated anti-rabbit antibody followed by avidin–β-galactosidase (41). (A) Stage IX. Staining is predominantly in step 9 spermatids. (B) Stages V and VI. Staining is predominantly in step 15 spermatids. (C) Stages X and XI. No staining is observed in the *nectin-2*$^{-/-}$ control cells. (D) Light micrograph of isolated condensed spermatid. (E) The same isolated condensed spermatid as in panel D, stained with anti-Nectin-2 monoclonal antibody 6B3 (1) and detected by immunofluorescence microscopy. (F) Spermatozoa from wild-type mice stained with anti-Nectin-2 monoclonal antibody 6B3 and detected by β-galactosidase activity. (G and H) Flow-cytometric analysis of Nectin-2 protein expression on epididymal sperm derived from *nectin-2*$^{+/+}$ mice (G) and *nectin-2*$^{-/-}$ mice (H). Analyses were performed with and without monoclonal antibody (mAb) 6B3. Ab, antibody. Magnifications: ×720 (A to C), ×4,000 (D and E), and ×3,000 (F).

phalloidin, a dye that specifically stains F-actin (15). Staining was observed throughout spermatozoa from wild-type mice, although it was most prominent in the middle piece (Fig. 6A). This staining pattern was seen in 92% (23 of 25 and 23 of 25) of the wild-type spermatozoa observed in two different experiments. In contrast, spermatozoa from *nectin-2*$^{-/-}$ mice stained mainly in the head, with relatively lower levels of staining occurring in the middle piece and the principal piece (Fig. 6B). This staining pattern was seen in 61 and 69% (11 of 18 and 22 of 32, respectively) of the spermatozoa observed in two

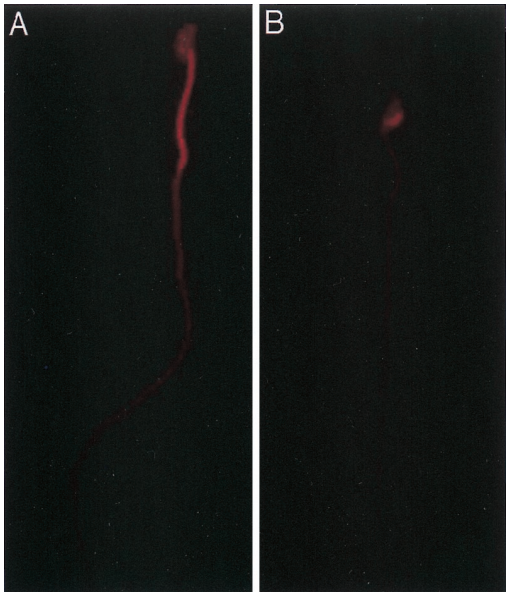

FIG. 6. Detection of F-actin in spermatozoa. Spermatozoa were stained with rhodamine phalloidin and photographed by fluorescence microscopy. (A) Spermatozoan from a wild-type mouse. The entire spermatozoan is stained, but the level of staining is highest in the middle piece. (B) Spermatozoan from a *nectin-2*$^{-/-}$ mouse. Staining is predominantly in the head.

different experiments. These results indicate that the distribution of F-actin in spermatozoa of wild-type mice differs from that seen in *nectin-2*$^{-/-}$ mice.

DISCUSSION

Spermatogenesis, the production of spermatozoa from precursor germ cells, is a complex process that requires tight regulation of developmental genes and extensive cellular restructuring. This process can be divided into three steps: spermatogonial renewal and proliferation, meiosis, and spermiogenesis (32). Spermatogonia proliferate and differentiate to generate diploid spermatocytes, which undergo two successive meiotic divisions to form haploid cells. During spermiogenesis the haploid cells restructure to form spermatozoa. Several morphogenic processes occur simultaneously during spermiogenesis, including condensation and nuclear shaping, development of an acrosome and a flagellum, reorganization of mitochondria, and elimination of residual cytoplasm.

In mice, mutation and disruption of numerous genes have been reported to affect various phases of spermatogenesis (33). For example, the spermatocytes of male mice that lack the transcriptional activator CREM (cyclic AMP-responsive element modulator) proceed to spermiogenesis, but then the spermatids fail to differentiate and there is an increase in the number of apoptotic germ cells (5, 28). Mice that lack calmegin, a testis-specific endoplasmic reticulum chaperone protein, produce morphologically normal spermatozoa which do not adhere to the zona pellucida of the egg (12). The genes of several structural proteins in the spermatid nucleus, which include transition proteins 1 and 2 and protamines 1 and 2, are transcribed and also translated in postmeiotic spermatids (10, 16, 17, 39). Premature translation of protamine 1 mRNA causes early nuclear condensation and arrests spermatid differentiation in mice (19), indicating that proper timing of gene expression may be critical for normal spermatogenesis. Such mouse models provide tools for gaining an understanding of the roles of various genes in the progression of spermatogonia to spermatozoa.

Here we report a block during late spermiogenesis in mice lacking *nectin-2*. Spermatozoa from *nectin-2*$^{-/-}$ mice have defects in nuclear and cytoskeletal morphology and in mitochondrial localization. The nuclear defect was observed beginning at step 11 of spermiogenesis. Mutant mice produce normal levels of motile sperm containing haploid DNA, demonstrating that spermatogonial renewal and proliferation and meiosis proceed normally in the absence of *nectin-2*. Histological examination of the testes from both wild-type and *nectin-2*$^{-/-}$ mice shows no differences that might suggest an arrest of development at early stages such as germ cell proliferation, meiosis, or steps 1 to 10 of spermiogenesis. Immunohistochemical analysis revealed that Nectin-2 is expressed only at the later steps of spermatid development (step 9 and beyond), which correlates with a putative role during cytoplasmic and nuclear restructuring.

Male mice lacking Nectin-2 may be infertile because the morphologically aberrant spermatozoa cannot reach, bind to, or penetrate the egg. Why does the lack of Nectin-2 lead to the production of morphologically abnormal spermatozoa? The abnormalities include misshapen nuclei with indentations, the presence of mitochondria in spermatozoan heads, and disorganization of mitochondrial helical sheaths and outer dense fibers in the middle piece. Cytoskeletal elements have been shown to be crucial in nuclear shaping and in the recruitment of mitochondria from the cytoplasm of the spermatid to the middle piece of the flagellum (26, 29, 34, 40). Therefore, the observed defects in spermatozoa from *nectin-2*$^{-/-}$ mice may be a consequence of cytoskeletal abnormalities. How might the lack of Nectin-2 affect cytoskeletal structure? Nectin-2 is a component of cell-cell anchoring junctions known as adherens junctions and is linked to F-actin through the actin filament-binding protein l-afadin (35). Anchoring junctions connect the cytoskeletal elements of neighboring cells, producing an extensive transcellular network that is structurally robust. In addition to their adhesive functions, adherens junctions are also believed to regulate cell shape and differentiation through signaling pathways. For example, other components of adherens junctions, the cadherins, are required for cellular rearrangements that occur during development (36). Like Nectin-2, cadherins are linked to F-actin by cytoplasmic proteins; the cadherin- and actin-binding proteins are called catenins. The effects of cadherins on development are mediated in part by signal transduction. Although the interaction of Ig-like cell adhesion molecules with the cytoskeleton is poorly understood, our results suggest that Nectin-2 regulates, directly or indirectly, cytoskeletal structure during spermiogenesis. This hypothesis is supported by the finding that the patterns of F-actin staining by rhodamine phalloidin differ in spermatozoa from wild-type and *nectin-2*$^{-/-}$ mice. In spermatozoa of wild-type mice, the staining is most intense in the middle piece. In spermatozoa of *nectin-2*$^{-/-}$ mice, the level of staining in the middle piece is noticeably lower than that in wild-type mice. These results suggest that the absence of Nectin-2 leads to reduced levels of F-actin in the middle piece. The details of how Nectin-2 influences the cytoskeleton remain to be elucidated. Expression of Nectin-2 during spermiogenesis might bring the l-afadin–F-actin complex to the middle piece and mediate structural changes of actin. These changes may be important in nuclear shaping, mitochondrial relocation, and outer dense fiber organization during spermiogenesis.

Nectin-2 is expressed on the plasma membrane in spermatids, and in spermatozoa it is expressed primarily on the middle piece. These observations suggest that Nectin-2 is relocated

during late spermiogenesis. The presence of Nectin-2 in the middle piece is intriguing in light of the defects in mitochondrial migration to the middle piece, the disorganization of the mitochondrial helix sheath, and the reduced levels of F-actin in the middle piece in *nectin-2*$^{-/-}$ mice. One possible explanation for the presence of Nectin-2 on the middle piece is that it is required for proper localization of F-actin, through the interaction with l-afadin. Disruption of the murine *afadin* gene leads to embryonic lethality (13). Studies of embryonic bodies derived from cultured ES cells revealed that the distribution of F-actin in cells lacking l-afadin differs from that in wild-type cells (13). Thus, changes in F-actin occur when either *nectin-2* or *afadin* is disrupted.

Nectin-2 is a homophilic adhesion molecule (1, 20, 35), and a purified soluble form of Nectin-2 lacking the transmembrane and cytoplasmic domains exists as a dimer (Dong and Racaniello, unpublished data). It is possible that Nectin-2 on spermatids interacts with Nectin-2 on other spermatids or on Sertoli cells. These interactions might be important for proper function of Nectin-2.

Although Nectin-2 expression is ubiquitous, *nectin-2*$^{-/-}$ mice have no overt defects other than infertility in males. Since the structural changes that occur during spermiogenesis are unique, it is possible that Nectin-2 function is not required in other tissues. Alternatively, Nectin-1, which is ubiquitously expressed, also binds l-afadin and might be expected to replace the function of Nectin-2 in other tissues.

The human *pvr* gene family currently consists of three members, *pvr*, *nectin-1*, and *nectin-2* (8, 21, 23). It is not known whether Pvr is a component of adherens junctions or whether it binds l-afadin; Pvr does not have an l-afadin-binding domain in the cytoplasmic region. In transgenic mice containing the human *pvr* gene, Pvr protein is expressed in the seminiferous epithelium in a pattern similar to that observed for Nectin-2 in mice (Dong and Racaniello, unpublished data). In addition, expression of *pvr* can partially overcome the morphological defects in spermatozoa of *nectin-2*$^{-/-}$ mice (Dong and Racaniello, unpublished data). These results are consistent with a role for *pvr* in spermatogenesis and suggest that Pvr, like Nectin-1 and Nectin-2, may interact with the cytoskeleton.

ACKNOWLEDGMENTS

M.J.B. and Y.D. made equal contributions to this paper.

We thank C. Pavel, T. DiChiara, J. Baker, A. Louvi, S. Zeitlin, T. Ludwig, A. Efstratiadis, S. Silverstein, R. Bohenzky, E. Lium, C. Panagiotidis, V. Papaioannou, C. S. H. Young, A. Stall, J. Rossant, E. Colston, and O. Flore for advice, discussions, and materials.

This work was supported by a grant (AI34418) to V.R. from the National Institutes of Health.

REFERENCES

1. **Aoki, J., S. Koike, H. Asou, I. Ise, H. Suwa, T. Tanaka, M. Miyasaka, and A. Nomoto.** 1997. Mouse homolog of poliovirus receptor-related gene 2 product, mPRR2, mediates homophilic cell aggregation. Exp. Cell Res. **235:** 374–384.
2. **Aoki, J., S. Koike, I. Ise, Y. Sato-Yoshida, and A. Nomoto.** 1994. Amino acid residues on human poliovirus receptor involved in interaction with poliovirus. J. Biol. Chem. **269:**8431–8438.
3. **Baker, J., M. P. Hardy, J. Zhou, C. Bondy, F. Lupu, A. R. Bellvé, and A. Efstratiadis.** 1996. Effects of an *Igf1* gene null mutation on mouse reproduction. Mol. Endocrinol. **10:**903–918.
4. **Bellvé, A.** 1993. Purification, culture and fractionation of spermatogenic cells. Methods Enzymol. **225:**84–113.
5. **Blendy, J. A., K. H. Kaestner, G. F. Weinbauer, E. Nieschlag, and G. Schütz.** 1997. Severe impairment of spermatogenesis in mice lacking the CREM gene. Nature **380:**162–165.
6. **Bradley, A.** 1987. Production and analysis of chimaeric mice, p. 113–151. *In* E. J. Robertson (ed.), Teratocarcinomas and embryonic stem cells: a practical approach. IRL Press, Oxford, United Kingdom.
7. **Chadeneau, C., B. LeMoullac, and M. G. Denis.** 1994. A novel member of the immunoglobulin gene superfamily expressed in rat carcinoma cell lines. J. Biol. Chem. **269:**15601–15605.
8. **Eberlé, F., P. Dubreuil, M. G. Mattei, E. Devilard, and M. Lopez.** 1995. The human PRR2 gene, related to the human poliovirus receptor gene (PVR), is the true homolog of the murine MPH gene. Gene **159:**267–272.
9. **Geraghty, R. J., C. Krummenacher, G. H. Cohen, R. J. Eisenberg, and P. G. Spear.** 1998. Entry of alphaherpesviruses mediated by poliovirus receptor-related protein 1 and poliovirus receptor. Science **280:**1618–1620.
10. **Hecht, N. B.** 1990. Regulation of 'haploid expressed genes' in male germ cells. J. Reprod. Fertil. **88:**679–693.
11. **Hogan, B., F. Costantini, and E. Lacy.** 1986. Manipulating the mouse embryo: a laboratory manual. Cold Spring Harbor Laboratory, Cold Spring Harbor, N.Y.
12. **Ikawa, M., I. Wada, K. Kominami, D. Watanabe, K. Toshimori, Y. Nishimune, and M. Okabe.** 1997. The putative chaperone calmegin is required for sperm fertility. Nature **387:**607–611.
13. **Ikeda, W., H. Nakanishi, J. Miyoshi, K. Mandai, H. Ishizaki, M. Tanaka, A. Togawa, K. Takahashi, H. Nishioka, H. Yoshida, A. Mizoguchi, S. Nishikawa, and Y. Takai.** 1999. Afadin: a key molecule essential for structural organization of cell-cell junctions of polarized epithelia during embryogenesis. J. Cell Biol. **146:**1117–1132.
14. **Johnson, R. S., B. M. Spiegelman, and V. E. Papaioannou.** 1992. Pleiotropic effects of a null mutation in the c-*fos* proto-oncogene. Cell **71:**577–586.
15. **Katanaev, V. L., and M. P. Wymann.** 1998. Microquantification of cellular and in vitro F-actin by rhodamine phalloidin fluorescence enhancement. Anal. Biochem. **264:**185–190.
16. **Kleene, K. C.** 1989. Poly(A) shortening accompanies the activation of translation of five mRNAs during spermiogenesis in the mouse. Development **106:**367–373.
17. **Kleene, K. C., R. J. Distel, and N. B. Hecht.** 1984. Translational regulation and deadenylation of a protamine mRNA during spermiogenesis in the mouse. Dev. Biol. **105:**71–79.
18. **Koike, S., I. Ise, Y. Sato, H. Yonekawa, O. Gotoh, and A. Nomoto.** 1992. A second gene for the African green monkey poliovirus receptor that has no putative N-glycosylation site in the functional N-terminal immunoglobulin-like domain. J. Virol. **66:**7059–7066.
19. **Lee, K., H. S. Haugen, C. H. Clegg, and R. E. Braun.** 1995. Premature translation of protamine 1 mRNA causes precocious nuclear condensation and arrests spermatid differentiation in mice. Proc. Natl. Acad. Sci. USA **92:** 12451–12455.
20. **Lopez, M., M. Aoubala, F. Jordier, D. Isnardon, S. Gomez, and P. Dubreuil.** 1998. The human poliovirus receptor related 2 protein is a new hematopoietic/endothelial homophilic adhesion molecule. Blood **92:**4602–4611.
21. **Lopez, M., F. Eberlé, M. G. Mattei, J. Gabert, F. Birg, F. Bardin, C. Maroc, and P. Dubreuil.** 1995. Complementary DNA characterization and chromosomal localization of a human gene related to the poliovirus receptor-encoding gene. Gene **155:**261–265.
22. **Mandai, K., H. Nakanishi, A. Satoh, H. Obaishi, M. Wada, H. Nishioka, M. Itoh, A. Mizoguchi, T. Aoki, T. Fujimoto, Y. Matsuda, S. Tsukita, and Y. Takai.** 1997. Afadin: a novel actin filament-binding protein with one PDZ domain localized at cadherin-based cell-to-cell adherens junction. J. Cell Biol. **139:**517–528. (Erratum, **139:**1060).
23. **Mendelsohn, C., E. Wimmer, and V. R. Racaniello.** 1989. Cellular receptor for poliovirus: molecular cloning, nucleotide sequence and expression of a new member of the immunoglobulin superfamily. Cell **56:**855–865.
24. **Morrison, M. E., and V. R. Racaniello.** 1992. Molecular cloning and expression of a murine homolog of the human poliovirus receptor gene. J. Virol. **66:**2807–2813.
25. **Morrison, M. E., H. Yuan-Jing, M. W. Wien, J. W. Hogle, and V. R. Racaniello.** 1994. Homolog scanning mutagenesis reveals poliovirus receptor residues important for virus binding and replication. J. Virol. **68:**2578–2588.
26. **Myles, D. G., and P. K. Hepler.** 1982. Shaping of the sperm nucleus in Marsilea: a distinction between factors responsible for shape generation and shape determination. Dev. Biol. **90:**238–252.
27. **Nagy, A., J. Rossant, R. Nagy, W. Abramow-Newerly, and J. C. Roder.** 1993. Derivation of completely cell culture-derived mice from early-passage embryonic stem cells. Proc. Natl. Acad. Sci. USA **90:**8424–8428.
28. **Nantel, F., L. Monaco, N. S. Foulkes, D. Masquiller, M. LeMeur, K. Henriksen, A. Dierich, M. Parvinen, and P. Sassone-Corsi.** 1997. Spermiogenesis deficiency and germ-cell apoptosis in CREM-mutant mice. Nature **380:**159–162.
29. **Olson, G. E., and V. P. Winfrey.** 1990. Mitochondria-cytoskeleton interactions in the sperm midpiece. J. Struct. Biol. **103:**13–22.
30. **Ren, R., and V. Racaniello.** 1992. Human poliovirus receptor gene expression and poliovirus tissue tropism in transgenic mice. J. Virol. **66:**296–304.
31. **Robertson, E. J.** 1987. Embryo-derived stem cell lines, p. 71–112. *In* E. J. Robertson (ed.), Teratocarcinomas and embryonic stem cells: a practical approach. IRL Press, Oxford, United Kingdom.
32. **Russell, L. D., R. A. Ettlin, A. P. Sinha Hikim, and E. D. Clegg.** 1990.

Histological and histopathological evaluation of the testis. Cache River Press, Clearwater, Fla.
33. **Sassone-Corsi, P.** 1997. Transcriptional checkpoints determining the fate of male germ cells. Cell **88:**163–166.
34. **Soley, J. T.** 1997. Nuclear morphogenesis and the role of the manchette during spermiogenesis in the ostrich (*Struthio camelus*). J. Anat. **190:**563–576.
35. **Takahashi, K., H. Nakanishi, M. Miyahara, K. Mandai, K. Satoh, A. Satoh, H. Nishioka, J. Aoki, A. Nomoto, A. Mizoguchi, and Y. Takai.** 1999. Nectin/PRR: an immunoglobulin-like cell adhesion molecule recruited to cadherin-based adherens junctions through interaction with Afadin, a PDZ domain-containing protein. J. Cell Biol. **145:**539–549.
36. **Uemura, T.** 1998. The cadherin superfamily at the synapse: more members, more missions. Cell **93:**1095–1098.
37. **Warner, M. S., R. J. Geraghty, W. M. Martinez, R. I. Montgomery, J. C. Whitbeck, R. Xu, R. J. Eisenberg, G. H. Cohen, and P. G. Spear.** 1998. A cell surface protein with herpesvirus entry activity (HveB) confers susceptibility to infection by mutants of herpes simplex virus type 1, herpes simplex virus type 2, and pseudorabies virus. Virology **246:**179–189.
38. **Williams, A. F., and A. N. Barclay.** 1988. The immunoglobulin superfamily—domains for cell surface recognition. Annu. Rev. Immunol. **6:**381–405.
39. **Yelick, P. C., Y. H. Kwon, J. F. Flynn, A. Borzorgzadeh, K. C. Kleene, and N. B. Hecht.** 1989. Mouse transition protein 1 is translationally regulated during the postmeiotic stages of spermatogenesis. Mol. Reprod. Dev. **1:**193–200.
40. **Yoshida, T., S. O. Ioshii, K. Imanaka-Yoshida, and K. Izutsu.** 1994. Association of cytoplasmic dynein with manchette microtubules and spermatid nuclear envelope during spermiogenesis in rats. J. Cell Sci. **107:**625–633.
41. **Zhang, S., and V. R. Racaniello.** 1997. Expression of PVR in intestinal epithelial cells is not sufficient to permit poliovirus replication in the mouse gut. J. Virol. **71:**4915–4920.